

Scanning magnetic imaging of Sr_2RuO_4

Per G. Björnsson,¹ Yoshiteru Maeno,² Martin E. Huber,³ and Kathryn A. Moler^{1,*}

¹*Geballe Laboratory for Advanced Materials and Department of Applied Physics, Stanford University, Stanford, California 94305-4045, USA*

²*Department of Physics and International Innovation Center, Kyoto University, Kyoto 606-8502, Japan*

³*Department of Physics, University of Colorado at Denver and Health Sciences Center, Denver, Colorado 80217-3364, USA*

(Received 14 March 2005; published 11 July 2005)

We magnetically imaged the ab -plane surface of single crystals of the unconventional superconductor Sr_2RuO_4 , including one sample with an array of microholes, using scanning superconducting quantum interference device and Hall probe microscopy in a dilution refrigerator at low applied magnetic fields. The images show dilute trapped vortices, as would be expected in conventional type-II superconductors, and no other magnetic features. We found no direct signs of the spontaneous magnetization that would be expected in a time-reversal symmetry-breaking (TRSB) superconductor. These measurements set upper limits on the presence of TRSB signatures in this material.

DOI: 10.1103/PhysRevB.72.012504

PACS number(s): 74.20.Rp, 74.70.Pq

I. INTRODUCTION

Strontium ruthenate, Sr_2RuO_4 (SRO), has been studied extensively since its superconducting properties were discovered in 1994.^{1,2} It was the first noncuprate superconductor with a layered perovskite structure to be discovered, eight years after the discovery of high- T_c in the cuprates. There has been a great effort to identify the structure of the energy gap.² The leading candidate is $\sin(ak_x) \pm i \sin(ak_y)$, which belongs to the same symmetry class as $k_x \pm ik_y$.³ One of the most dramatic implications of this order parameter candidate is the time-reversal symmetry-breaking (TRSB) nature of this symmetry group. The TRSB implies that SRO should have spontaneous currents flowing at boundaries and around defects in its ground state. The report by Luke *et al.* of a muon spin rotation signal characteristic of “a broad distribution of fields arising from a dilute distribution of sources”⁴ is the earliest and still the main evidence for TRSB. Further supporting evidence for a two-component order parameter comes from the details of the flux lattice, as observed by Kealey *et al.* with neutron scattering.⁵

Phase-sensitive measurements performed recently by Nelson *et al.*⁶ have added data indicating that the superconducting order parameter changes sign under inversion, which is very strong evidence of odd-parity superconductivity. Thus, the issue of the parity of the order parameter appears to be settled, and one of the last few remaining pieces in the puzzle of the Sr_2RuO_4 wave function is an experiment that can directly probe the effects of TRSB, such as directly measuring the spatial distribution of the expected spontaneously generated magnetic fields.

There are three magnetic signatures of TRSB that are observable by local magnetic imaging. (1) *Edge currents*. In a single crystal with no domains (e.g., the order parameter throughout the crystal would be either $k_x + ik_y$ or $k_x - ik_y$), there should be an edge current within a coherence length of the edge, and a counter-circulating shielding current within a penetration depth.^{7,8} Kwon *et al.* argued that in Sr_2RuO_4 , this effect would produce a magnetic flux of 2.6 G μm per unit

length of the edge.⁸ (2) *Currents at domain walls*. Matsuzono and Sigrist argued that domains are energetically unfavorable, and are only found because of domain wall pinning.⁹ In principle, the domain size may range from the sample size to the coherence length, $\xi_{ab} = 66$ nm. Very different patterns of current flow would result depending on whether the domains are smaller or larger than the penetration depth, $\lambda_{ab} \approx 200$ nm. We are not aware of quantitative theoretical predictions on the expected magnetic signal from domain walls. (3) *Defects*. Currents with counter-circulating shielding currents are also expected to flow around defects.

In previous work, Tamegai *et al.* studied local magnetization at the edge of a sample using a stationary $5 \times 5 \mu\text{m}^2$ Hall probe.¹⁰ They detected no spontaneous magnetic fields associated with edge currents, although they did report anomalies in the magnetization hysteresis loops that they suggest indicate the presence of chiral domains. Using scanning superconducting quantum interference device (SQUID) imaging, Dolocan *et al.* observed coalescing vortices forming flux domains, which they suggest indicate the presence of topological defects such as domain walls resulting from unconventional chiral superconductivity.¹¹ However, they did not detect, nor were they explicitly looking for, magnetization signals from edges and defects.

In this paper, we report on imaging an as-cleaved crystal using a scanning SQUID with a 4 μm diameter pickup loop,¹² and a second cleaved crystal with an array of patterned microholes using a scanning Hall probe with a lithographically defined active area of $0.5 \times 0.5 \mu\text{m}^2$.¹³ The crystal with patterned holes gives us the controlled edge structure that should be ideal for detecting TRSB signals, since the largest effects have been predicted at edges. We do not observe edge currents or chiral domains.

II. EXPERIMENT

The instrument used for the scanning magnetic measurements is a scanning probe microscope in a dilution refrigerator.^{14,15} The entire experimental area is magnetically

shielded by three layers of high-permeability magnetic shielding around the Dewar, and a 300 G magnet is wound around the vacuum can. The residual field in all three directions is generally of order 50 mG. However, a larger residual field, as large as 1 G, may result from flux trapping in the indium seal in the mixing chamber after a large field has been applied.

Either a Hall probe or a SQUID may be mounted as the scanned probe. The active area of the sensor is located within a distance l of a corner of the sensor chip. l is typically 8 and 20 μm in our present generation of Hall probes and SQUIDs, respectively. The sensor chip is aligned at room temperature at a shallow angle θ with respect to the sample, such that the minimum experimental height h of the active area is given by $h=l \sin \theta$. We typically fly the sensor a few hundred nanometers above the minimum height in order to avoid sample heating, electrical shorting, and piezoresistive effects in the case of the Hall probe. The SQUIDs provide high flux sensitivity, with a noise floor of $1 \mu\Phi_0/\sqrt{\text{Hz}}$, but average over a relatively large area, $\sim 17 \mu\text{m}^2$. The lithographically defined active area of the Hall probe used here was $\sim 0.25 \mu\text{m}^2$, but in these measurements the effective spatial resolution of the Hall probe was limited by its height above the sample, $\sim 1 \mu\text{m}$. The noise level of submicron Hall probes is generally limited by $1/f$ noise. The Hall probe used here had a noise level of $80 \text{ mG}/\sqrt{\text{Hz}}$ at 1 Hz. To put the figures of merit in comparable units, the SQUIDs have a white noise floor of $1.2 \mu\text{G}/\sqrt{\text{Hz}}$ in a uniform magnetic field. However, determining the field sensitivity in a nonuniform field is complicated by the shape of the pickup region.

The Sr_2RuO_4 samples used were single crystals, grown by a floating-zone method.¹⁶ T_c as determined by bulk ac susceptibility measurements on pieces from the same crystal bar was 1.422 K with a transition width of 24 mK. This T_c agrees with the less precise observations of T_c —close to 1.5 K—in our scanning measurements. The crystals were cleaved before imaging, and no further surface treatment such as polishing was done. In one crystal, we patterned an array of approximately 1 μm holes with a spacing of 20 μm using a focused ion beam (FIB). A scanning electron microscope (SEM) image of this sample is shown in Fig. 1. Each sample was mounted in silver epoxy and connected to the mixing chamber baseplate of the dilution refrigerator with a copper wire for thermal contact.

A. SQUID imaging

In our SQUID images of an unpatterned sample, acquired at a height of approximately 2 μm above the sample surface, in images where the background field was carefully compensated so that there were no vortices in the field of view, we detected a smoothly varying background and a few dipole-like artifacts that were present even at 4 K and thus must be unrelated to the superconductivity of the Sr_2RuO_4 sample. The smooth background appears to be caused by pickup from a secondary pickup loop, which was extended over the edge of the sample. The total magnitude of the background variation is on the order of 50 mG, and the noise level in the

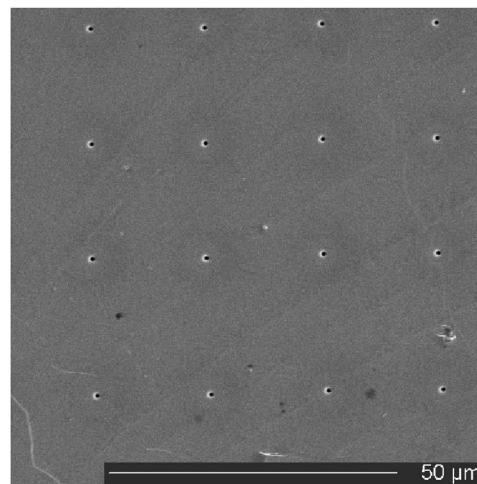


FIG. 1. A SEM image of the Sr_2RuO_4 crystal used for the Hall probe imaging. An array of holes was milled in the sample using a FIB. The hole spacing is 20 μm .

measurements, measured as the rms difference between adjacent pixels with 0.6 μm spacing, is 0.45 mG.

B. Hall probe imaging of a patterned sample

Our next experiment used a Hall probe with an active area of $0.5 \mu\text{m} \times 0.5 \mu\text{m}$ to image a crystal with FIB-milled holes (Fig. 1). This experiment had three improvements that allow the data to be compared semiquantitatively with theory. First, the FIB-milled holes provide edges throughout the imaged area. Second, the Hall probe has only a single active area and therefore does not suffer the same systematic background errors. Third, the Hall probe has a smaller active area than the SQUID and can be scanned at a lower height, providing higher spatial resolution.

A low-field Hall probe scan of the sample taken at $T=100 \text{ mK}$ is shown in Fig. 2. The image is completely free of features other than a few isolated trapped vortices, such as commonly appear in low-field, low-temperature magnetic scans of type-II superconductors. These vortices appear to be entirely conventional, carrying a magnetic flux of $h/2e$ within 10% error, as determined by integration of the measured local magnetic field. The apparent lateral extent and shape of the vortices is limited by the sensor scan height. Fits to these images of isolated individual vortices determine the probe height to be $1.2 \pm 0.2 \mu\text{m}$ above the surface. Thus, our spatial resolution is limited by the height of the probe above the surface, not by the probe size itself.^{17,18}

The dominant noise source in these measurements is Hall probe $1/f$ noise. To minimize this noise, we used the standard scanning microscopy technique of scanning relatively quickly (2 s/scan line) and averaging multiple scans, subtracting the background level of each line. For the image in Fig. 2, 80 scans were averaged. The resulting background noise has an rms value of 35 mG, with no sign of the array of holes milled in the sample or any other features.

Scanning Hall probe images were also made after cooling the sample through T_c in fields up to 10 G, staying well below H_{c1} . A series of images in this field range are shown in

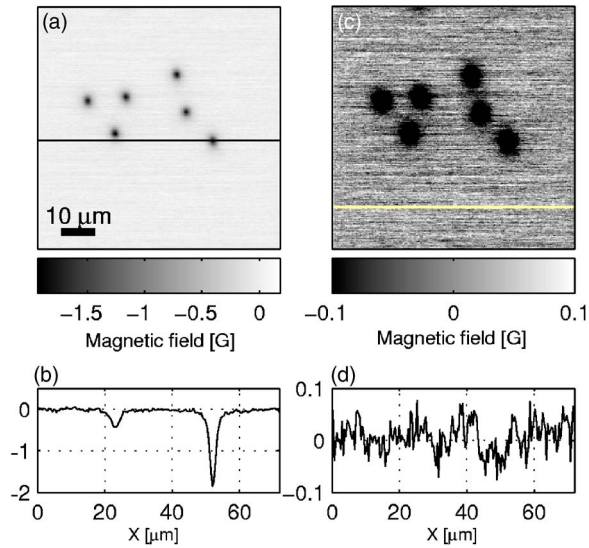


FIG. 2. (Color online) Scanning Hall probe image at $T=100$ mK of the sample shown in Fig. 1, cooled in a background field of ~ 25 mG. The background has been line normalized to remove $1/f$ noise. (a) Image with a color scale showing the full measured magnetic field range. Isolated trapped vortices dominate the image. (b) Cross section taken along the darkened line in (a). (c) Image with an expanded color scale, showing that there are no obvious features in the noise. (d) Cross section taken along the lightened line in (c).

Fig. 3. The measurement temperature for these scans was 100 mK. With these applied fields, we would expect to see isolated trapped vortices. The most striking feature in the images is that the vortex distribution looks very inhomogeneous. In addition, in the densely populated areas, the vortices appear to form lines. We have not observed (optically or using SEM) any imperfections or structure in the crystal on length scales that correspond to these lines, although we cannot entirely rule out some kind of damage, possibly from the FIB patterning. We note, however, that even for the densely populated vortex images, for example, for 5 G, the location of the FIB holes is not evident. This indicates that the FIB patterning does not damage the superconductivity and furthermore the holes with micron-scale depth do not act as strong pinning centers for the vortices.

The vortex structure that we detected in the measurements in moderate fields is similar to the structures seen by Dolocan *et al.*,¹¹ in that the vortices group already in small perpendicular fields. However, we find that the vortices order in lines without any applied in-plane field (other than any residual field in the magnetically shielded Dewar or an in-plane field caused by the field inhomogeneity of our magnet, both of which should be small compared to the applied perpendicular field). On the other hand, Dolocan *et al.* saw the vortex pattern evolving from irregularly shaped flux domains to a line-like structure with increasing applied in-plane fields; in order to obtain a line-like structure, they need to apply in-plane fields that are much larger than the applied perpendicular field. There is a possibility that sample differences play a significant role; they report that $T_c = 1.35 \pm 0.05$ K, which is lower than our T_c . The T_c of

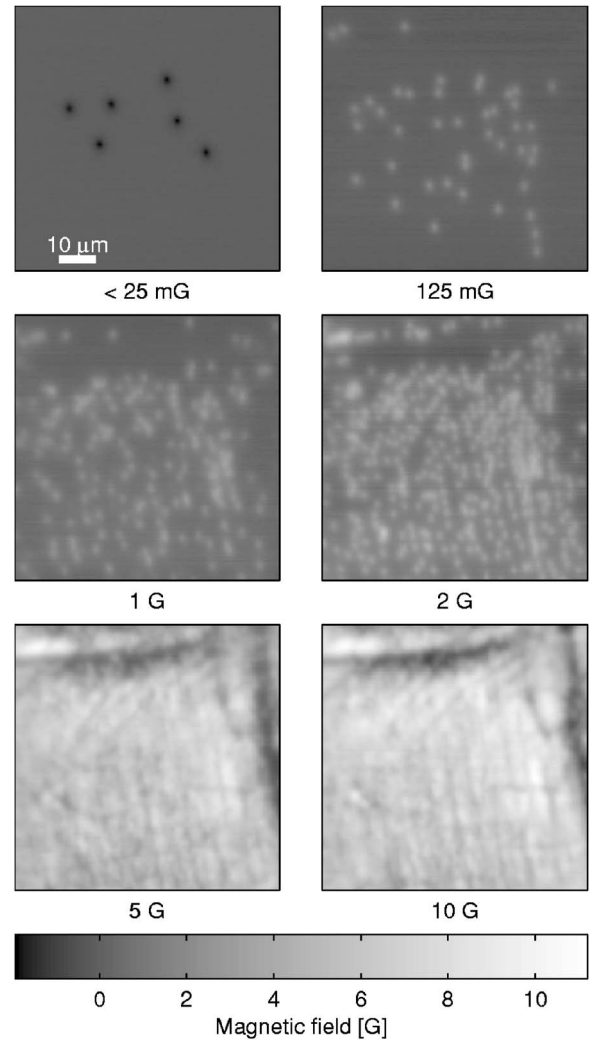


FIG. 3. Hall probe scans at $T=100$ mK of a sample field-cooled in moderate magnetic fields. The vortices appear to form lines that are spaced much more closely than the FIB-milled hole pattern. There are also regions at the top and right-hand side of the imaged area in which the density of vortices is much lower than the average in the images.

Sr_2RuO_4 is very sensitive to sample purity.² For further investigation of this effect, high-resolution measurements on high-quality unpatterned samples are important, since this would rule out sample patterning effects and allow measurement in a wider range of fields.

III. DISCUSSION

In the remainder of the paper, we discuss the implications of our observations in the context of theoretical predictions and estimates for signatures of TRSB superconductivity. One way to quantify the nondetection of edge currents is to consider the field generated by a current loop. A circulating current around a $1 \mu\text{m}$ diameter hole would give a measured signal of approximately $1 \text{ mG}/\mu\text{A}$ at our measurement height. Thus, the measurements set a limit on net circulating currents of less than $35 \mu\text{A}$. The total edge current and

counter-circulating shielding current could each be considerably larger.

We can also compare our nonobservation of edge currents at microholes to the calculation by Kwon, Yakovenko, and Sengupta for magnetic flux resulting from edge currents.⁸ Naïvely, the predicted magnetic flux of 2.6 G μm per unit length of edge should fall off like the inverse of the height, leading to a magnetic field of slightly under 1 G at a height of 1 μm . Although a self-consistent calculation including Meissner effects in three dimensions for our specific geometry is necessary to make truly quantitative comparisons, this naïve estimate for TRSB is well above our noise level of 35 mG.

Our nonobservation of edge currents could be explained in three ways: either the preceding estimate for TRSB edge currents is insufficient, there are multiple chiral domains on the length scale of the microholes, or the material is not TRSB. It is therefore important to understand the possible structure and magnetic signature of chiral domains.

If the size of the domains is much larger than λ_{ab} , the magnetic moment should be shielded in the interior of the domains and the only measurable signal should come from domain walls. Both the shielding currents and the neighboring domains would lead to a cancelation of the signal when measured at a height that is large compared to ξ_{ab} and λ_{ab} , but setting quantitative limits on currents at domain walls requires a specific theoretical model.

If the size of the domains is on the order of λ_{ab} or smaller, the magnetic moment will not be fully shielded in the interior of the domain. Signals of opposite sign from neighboring domains will cancel out rapidly with sensor height or size. The signal at a given height from many domains can be estimated as follows. If the magnetic field at the sample surface is Fourier transformed into its spectral components

$B_z(\vec{k}, z=0)$, where \vec{k} is the spatial wave vector in the plane of the sample surface, then the amplitude of each spectral component at the height z above the surface will be decreased by a factor of e^{-kz} .¹⁹ The actual measurable field would be strongly dependent on the distribution of domain sizes; a perfect checkerboard pattern with identically sized domains would give extremely rapid cancelation, but a distribution with some spread in the domain size distribution would have lower-frequency components which would propagate further in the z direction. The actual expected field is thus strongly model dependent, primarily influenced by the average and standard deviation of the domain sizes; lacking a model that predicts these parameters, it is impossible to make strong predictions for the external magnetic field.

IV. CONCLUSIONS

In summary, using scanning SQUID imaging of an unpatterned Sr_2RuO_4 sample and Hall probe imaging of a sample with FIB-milled micro holes we have not detected any sign of spontaneous magnetization which should arise from a TRSB order parameter. More detailed theoretical modeling and measurements with smaller sensors closer to the sample both appear vital to resolving this issue.

ACKNOWLEDGMENTS

We thank P. A. Lee, B. Braunecker, D. Agterberg, A. P. Mackenzie, M. Sigrist, H. Yaguchi, H. Bluhm, and G. Luke for fruitful discussions on theory and implications of earlier measurements on Sr_2RuO_4 , J. W. Guikema for fabricating the Hall probes used for the measurements, and Z. Q. Mao for his contribution to the crystal growth. Funding for this project was provided by the DOE, the NSF, JSPS, and MEXT.

*Electronic address: kmoler@stanford.edu

¹Y. Maeno, H. Hashimoto, K. Yoshida, S. Nishizaki, T. Fujita, J. G. Bednorz, and F. Lichtenberg, *Nature (London)* **372**, 532 (1994).

²A. P. Mackenzie and Y. Maeno, *Rev. Mod. Phys.* **75**, 657 (2003).

³K. Deguchi, Z. Q. Mao, H. Yaguchi, and Y. Maeno, *Phys. Rev. Lett.* **92**, 047002 (2004).

⁴G. M. Luke *et al.*, *Nature (London)* **394**, 558 (1998).

⁵P. G. Kealey *et al.*, *Phys. Rev. Lett.* **84**, 6094 (2000).

⁶K. D. Nelson, Z. Q. Mao, Y. Maeno, and Y. Liu, *Science* **306**, 1151 (2004).

⁷M. Sigrist and K. Ueda, *Rev. Mod. Phys.* **63**, 239 (1991).

⁸H. J. Kwon, V. M. Yakovenko, and K. Sengupta, *Synth. Met.* **133**, 27 (2003).

⁹M. Matsumoto and M. Sigrist, *J. Phys. Soc. Jpn.* **68**, 994 (1999).

¹⁰T. Tamegai, K. Yamazaki, M. Tokunaga, Z. Mao, and Y. Maeno, *Physica C* **388–389**, 499 (2003).

¹¹V. O. Dolocan, C. Veauvy, Y. Liu, F. Servant, P. Lejay, D. Mailly, and K. Hasselbach, *cond-mat/0406195* (to be published).

¹²M. E. Huber *et al.* (unpublished).

¹³J. W. Guikema and K. A. Moler (unpublished).

¹⁴P. G. Björnsson, B. W. Gardner, J. R. Kirtley, and K. A. Moler, *Rev. Sci. Instrum.* **74**, 4153 (2001).

¹⁵P. G. Björnsson, M. E. Huber, and K. A. Moler, *Physica B* **329–333**, 1491 (2003).

¹⁶Z. Q. Mao, Y. Maeno, and H. Fukazawa, *Mater. Res. Bull.* **35**, 1813 (2000).

¹⁷A. M. Chang, H. D. Hallen, L. Harriott, H. F. Hess, H. L. Kao, R. E. Miller, R. Wolfe, and J. van der Ziel, *Appl. Phys. Lett.* **61**, 1974 (1992).

¹⁸J. R. Kirtley, V. G. Kogan, J. R. Clem, and K. A. Moler, *Phys. Rev. B* **59**, 4343 (1999).

¹⁹B. J. Roth, N. G. Sepulveda, and J. John P. Wickswo, *J. Appl. Phys.* **65**, 361 (1989).